Autologous Cardiomyotissue Implantation Promotes Myocardial Regeneration, Decreases Infarct Size, and Improves Left Ventricular Function

Joanna J. Wykrzykowska, MD*; Audrey Rosinberg, MD*; Seung U. Lee, MD; Pierre Voisine, MD; Guifu Wu, MD, PhD; Evan Appelbaum, MD; Munir Boodhwani, MD; Frank W. Sellke, MD; Roger J. Laham, MD

Background—Cell therapy for myocardial infarction (MI) may be limited by poor cell survival and lack of transdifferentiation. We report a novel technique of implanting whole autologous myocardial tissue from preserved myocardial regions into infarcted regions.

Methods and Results—Fourteen rats were used to optimize cardiomyotissue size with peritoneal wall implantation (300 μm identified as optimal size). Thirty-nine pigs were used to investigate cardiomyotissue implantation in MI induced by left anterior descending balloon occlusion (10 animals died; male-to-female transplantation for tracking with in situ hybridization for Y chromosome, n=4 [2 donors and 2 MI animals]; acute MI implantation cohort at 1 hour, n=13; and healed MI implantation at 2 weeks, n=12). Assessment included echocardiography, magnetic resonance imaging, hemodynamics, triphenyltetrazolium chloride staining, and histological and molecular analyses. Tracking studies demonstrated viable implants with donor cells interspersed in the adjacent myocardium with gap junctions and desmosomes. In the acute MI cohort, treated animals compared with controls had improved perfusion by magnetic resonance imaging (1.2±0.01 versus 0.86±0.05; $P<0.01$), decreased MI size (magnetic resonance imaging: left ventricle, 2.2±0.5% versus 5.4±1.5%, $P=0.04$; triphenyltetrazolium chloride: anterior wall, 10.3±4.6% versus 28.9±5.8%, $P<0.03$), and improved contractility (dP/dt, 1235±215 versus 817±817; $P<0.05$). In the healed MI cohort, treated animals had less decline in ejection fraction between 2 and 4 week assessment (−3±4% versus −13±−4%; $P<0.05$), less decline in ±dP/dt, and smaller MI (triphenyltetrazolium chloride, 21±11% versus 3±8%; $P=0.006$) than control animals. Infarcts in the treated animals contained more mdr-1$^+$ cells and fewer c-kit$^+$ cells with a trend for decreased expression of matrix metalloproteinase-2 and increased expression of tissue inhibitor of metalloproteinase-2.

Conclusion—Autologous cardiomyotissue implanted in an MI area remains viable, exhibits electromechanical coupling, decreases infarct size, and improves left ventricular function. **(*Circulation*. 2011;123:62-69.)**

Key Words: myocardial infarction ■ remodeling ■ stem cells

Myocardial infarction (MI) and its resultant left ventricular (LV) dysfunction remain a leading cause of mortality and morbidity. Different therapies for myocardial regeneration have been investigated with varying results and no definitive beneficial effects.[1–11] Concomitantly, the intrinsic regenerative potential of the myocardium has been increasingly recognized.[12–14] Adult cardiac stem cells injected into vasculature of rats after MI are able to differentiate into cardiomyocytes and arterioles.[15,16] In addition, it has been increasingly recognized that the delivery modality is a key limiting step in attempts at myocardial regeneration and angiogenesis with poor survival of transplanted cells (possible related to "milieu") and limited deposition and retention of injected cytokines.[17–20] This, coupled with mounting evidence relative to the lack of transdifferentiation potential of adult non–cardiac-derived stem cells, warrants a novel approach to myocardial regeneration.[21,22]

Clinical Perspective on p 69

We have developed a novel approach to adult cardiomyocyte transplantation. In a porcine model of MI, core biopsies of myocardial tissue are obtained from the preserved basal ventricular septum and used for implantation into the myocardial scar

Received January 28, 2006; accepted October 8, 2010.

From the Cardiology Division (J.J.W., G.W., E.A., R.J.L.) and Cardiovascular Surgery (M.B., F.W.S.), Beth Israel Deaconess Medical Center, Harvard Medical School, Boston MA; Division of Cardiac Surgery, Lenox Hill Hospital, New York, NY (A.R.); Kwangju Christian Hospital, Gwangju, Korea (S.U.L.); Hopital Laval, Quebec, QC, Canada (P.V.); and Interventional Cardiology, Thoraxcenter, Erasmus Medical Center, Rotterdam, the Netherlands (J.J.W.).

*Drs Wykrzykowska and Rosinberg contributed equally to this article.

Guest Editor for this article was Shigetake Sasayama, MD.

The online-only Data Supplement is available with this article at http://circ.ahajournals.org/cgi/content/full/CIRCULATIONAHA.108.832469/DC1.

Correspondence to Roger J. Laham, MD, Beth Israel Deaconess Medical Center, Harvard Medical School, 330 Brookline Ave, Boston, MA 02215. E-mail rlaham@bidmc.harvard.edu

Circulation **is available at http://circ.ahajournals.org** **DOI: 10.1161/CIRCULATIONAHA.108.832469**

with their intact milieu and without the need for tissue culture and processing. Here, we present the results of preclinical studies for this new technique in the treatment of MI.

Methods

All experiments were performed in accordance with National Institutes of Health guidelines and were approved by the Institutional Animal Care and Use Committee at Beth Israel Deaconess Medical Center.

Myotissue Sizing Experiments

Fourteen inbred rats (50 to 60 g) were used. Donor rats (n=3) were euthanized with CO_2 inhalation, and the heart was excised and placed in normal saline. Strips of varying diameters (100 to 500 μmol/L) were obtained under a dissecting microscope. Eleven rats were then anesthetized with intraperitoneal ketamine/xylaxine (0.1 mL /100 g). The abdominal skin was incised and rectus muscle was exposed. Strips were implanted, and rectus fascia was closed with 10–0 Prolene suture. Animals were divided into 5 groups (n=2 per group) with implantation of 100-, 200-, 300-, 400-, and 500-μm strips (1 strip per animal). The animals were allowed to recover and were euthanized after 1 week, and the abdominal wall was formalin fixed, paraffin embedded, and sectioned for hematoxylin and eosin staining.

Porcine Balloon Occlusion Catheter Model of Anterior MI

Thirty-nine 30- to 40-kg Yorkshire pigs were anesthetized with intramuscular ketamine (10 mg/kg) and isoflurane (2 normal animals as donors for male-to-female transplantation and 37 infarcted animals: 13 animals for acute infarct study, 12 animals for healed infarct study, 2 recipient animals for tracking experiments, and 10 animals died during balloon occlusion of intractable ventricular fibrillation before being randomized, leading to more aggressive pretreatment with Mg, KCl, metoprolol, and lidocaine). A 2.75×20-mm angioplasty balloon (Maverick, Boston Scientific, MA) was advanced over the wire and positioned in the mid left anterior descending artery after the takeoff of the first diagonal branch. The balloon was inflated to 6 atm for 60 minutes to produce an anterior MI. Balloon occlusion and Thrombolysis in Myocardial Infarction grade 0 flow were confirmed with contrast injection. The balloon was deflated after a minimum of 60 minutes of uninterrupted occlusion, and the surviving animals were allowed to recover. LV angiography was performed in all animals to confirm the presence of anterior wall motion abnormality.

Septal Biopsy and Myotissue Implantation Into Myocardial Scar Tissue

Implantations were performed acutely in acute MI cohort and 2 weeks after the initial infarction (ie, after the period of acute inflammation when scar formation and remodeling process have ensued in the healed infarct cohort). A right anterior thoracotomy through the fourth intercostal space was performed. The pericardium was opened and the lung retracted. The right ventricular free wall was incised, and a short 8F sheath (Cordis) was inserted and secured with a purse string suture. A liver bioptome (Cook Inc, Bloomington, IN) was inserted via an 8F sheath into the right ventricle and aimed at the basal septum under fluoroscopic guidance. Between 6 and 10 core biopsies (average, 9) were obtained with the bioptome from the basal septum. The anterior wall was exposed by rotating the heart slightly with a sponge stick. Six biopsies were then implanted into the anterior wall of the LV 0.5 cm distal to the left anterior descending artery and D1 bifurcation (visually identified). This was done by unloading the liver bioptome (Cook Inc) and rotating it in situ so as not to remove the implanted biopsy material (see the online-only Data Supplement for a detailed description). In each cohort, animals were randomized to cardiomyotissue implantation or sham injections. Sham animals also underwent the septal biopsy. The empty liver bioptome without the implant tissue was then introduced into the anterior wall.

In Situ Hybridization of the Y Chromosome for Implant Viability Assessment

Four sibling pairs of male and female pigs were used for this experiment. Two animals died during MI induction, leaving 2 animals for implantation. Two weeks later, the female recipients were brought back with their male siblings. Male hearts were harvested via median sternotomy, and basal septal biopsies were immediately taken after opening of the right ventricular cavity. Cardiomyotissue from the basal septum of the male sibling was implanted into the anterior wall myocardial infarct area of the females under direct vision. The area of implantation (9 to 11 implants per animal) was demarcated with 6–0 Prolene sutures. The female recipients received 3 days of pulse dose steroids (40 mg or 1 mg/kg) and 10 mg thereafter to prevent rejection (not HLA matched). The hearts of the recipients were harvested 2 weeks after implantation and 4 weeks after the initial MI. In situ hybridization for Y chromosome was performed on the harvested female recipient hearts to quantify the number of viable implants. Hybridization with Starfish biotinylated pig Y chromosome DNA probe (Cambio, Guildford, Surrey, UK) was performed overnight at 37° C in a humidified chamber. A streptavidin-biotin system with diaminobenzidine development (Vector, Burlingame, CA) followed by hematoxylin counterstaining was used to visualize male cells.

Infarct Volume, Myocardial Perfusion, and Functional Assessment by Cardiac Magnetic Resonance

Animals in the acute MI cohort underwent cardiovascular magnetic resonance on a 1.5-T General Electric TwinSpeed Scanner (GE Healthcare Technologies, Milwaukee, WI) 4 weeks after infarction as previously described.[23] The following evaluations were performed: extent of myocardial necrosis/infarction defined by the volume of myocardium demonstrating hyperenhancement on delayed contrast imaging, resting regional and global LV systolic function, and resting first-pass regional myocardial perfusion.

Functional Assessment of LV Function by Echocardiography (Transthoracic and Epicardial)

In the healed infarct cohort, 2 weeks after MI, baseline 2-dimensional and 2- dimensional–directed M-mode epicardial echocardiography was performed in multiple views (standard short-axis and long-axis views, as well as epicardial views)[24] to assess LV ejection fraction (EF) and LV end-diastolic dimension.[25] Transthoracic echocardiography was performed before implantation with the animal chest closed. Epicardial echocardiography windows were obtained before implantation after the chest was open. Magnetic resonance imaging (MRI) was not performed because of multiple procedures in this cohort to reduce time under anesthesia. End-systolic and end-diastolic LV cavity dimensions at the level of midpapillary muscles were determined in the M mode. EF was calculated from the M-mode–derived cavity dimensions in the Teicholz formula: (end-diastolic dimension−end-systolic dimension)/end-diastolic dimension×100. Measurements were repeated at 4 weeks after infarction at the time of tissue harvest. In the acute cohort, echocardiography was performed at the time of death (at 4 weeks). Echocardiographic analysis was performed quantitatively and qualitatively by 2 experienced echocardiographers in a blinded fashion.

Hemodynamic Assessment

LV pressure was measured with a high-fidelity micromanometer catheter placed in the LV cavity in a retrograde fashion. The rate of change of LV pressure was measured and averaged over 10 beats (dP/dt). Left atrial pressure was measured with a 3.5-JL 5F catheter advanced (retrograde) to left atrium. All data were recorded digitally and stored for offline analysis (Sonosoft, Sonometrics Corp, London, ON, Canada).

Histology, Morphometric Analysis, and Immunohistochemistry

Four weeks after the initial infarction, animals were euthanized under general anesthesia, and the hearts were harvested and cut into 5 transverse slices. The apical and middle slices were used for myocardial viability with 1% triphenyltetrazolium chloride (TTC) in phosphate buffer (Sigma Chemical) and incubated for 20 minutes at 38°C as previously described.[25,26] Stained slices were placed on clear acetate glass, and the infarct area was measured by planimetry (by 2 independent observers). The remaining cardiac tissue was placed in 10% formalin for paraffin embedding and processed for immunohistochemistry staining. Tissue was also snap-frozen in liquid nitrogen at −80°C for subsequent protein and RNA analyses (for matrix metalloproteinase-2 [MMP-2] and tissue inhibitor of metalloproteinase-2 [TIMP-2] expression). Paraffin tissues were subjected to antigen retrieval techniques (immersion in boiling citrate buffer). Immunohistochemistry was performed with mdr-1 at 1:40 dilution (Chemicon International, Temecula, CA), c-kit at 1: 200 dilution (Dako, Carpinteria, CA),[27] anti-connexin 43 (Zymed, San Francisco, CA) at 1:250 dilution, anti–pan-cadherin (Zymed) at 1:250 dilution, and platelet endothelial cell adhesion molecule-1 (PECAM-1) at 1:250 dilution (Santa Cruz Biotechnology, Inc, Santa Cruz, CA). Apoptotic cells were visualized with terminal deoxynucleotidyl transferase dUTP nick-end labeling (TUNEL) assay as previously described[18] (Apotag kit, Chemicon). Anti-isotype secondary antibodies (dilution, 1:250) and a streptavidin-biotin system with a diaminoxybenzidine development system was used to visualize the "stem" cells and PECAM-1$^+$ cells. Sections were counterstained with hematoxylin. Cells were counted with image analysis software (SpotAdvanced, Sterling Heights, MI; 10 representative ×10-power fields for stem cells and 10 ×40-power fields for PECAM-1), and assessment was blinded to treatment assignment. Data are presented as the average number of cells per 1 mm^2.

Molecular Studies

Myocardial tissue samples were lysed in radioimmunoprecipitation assay solution (Boston Bioproducts, Ashland, MA). Protein concentrations were determined by Bradford assay. Equal amounts of protein were subjected to fractionation on 10% SDS-polyacrylamide under reducing conditions. Protein extracts were transferred to polyvinylidene difluoride membranes (Millipore, Bedford, MA). MMP-2 and TIMP-2 (Chemicon) were detected with specific antibodies. Immunoblots were visualized with appropriate secondary antibodies conjugated to horseradish peroxidase and chemiluminescence detection reagents (Amersham, Life Science, Arlington Heights, IL). Values of image densitometry were obtained with ImageJ software and adjusted by the ratio of sample loading as determined by Ponceau Red staining.

Statistical Analysis

Data analysis and graphing were performed with the Statview software package (SAS Institute Inc, Cary, NC). Groups were compared through the use of 2-tailed Student t test with a cutoff for statistical significance of $P=0.05$. For comparisons of data at 2 and 4 weeks, paired t tests were used to compare means within groups, whereas unpaired tests were used to compare mean changes between groups. Normal distribution of the data was verified before parametric analysis was performed. Correction was made for multiple comparisons. Data are expressed as mean±SD.

Results

Sizing Experiments

Abdominal wall sections were obtained from implanted rats. Tissues ≤300 μm remained viable at 1 week after implantation in all animals. Tissues 400 and 500 μm in diameter showed necrosis, indicating that the maximal tissue size for implantation would be 300 μm, probably related to revascularization of the implant (Figure 1).

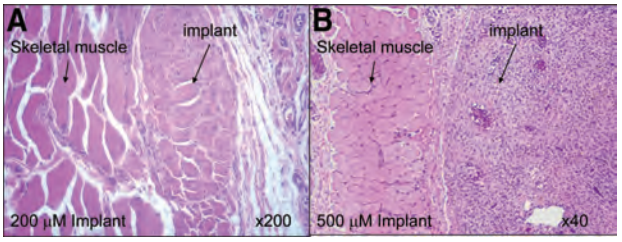

Figure 1. Sizing experiments. A, Myocardial tissue ≤300 μm remained viable next to skeletal myocytes of the rectus muscle. Myocardial architecture was preserved (×200). B, Myocardial tissue necrosis in strips 400 and 500 μm in diameter next to the rectus muscle with loss of myocardial architecture (×40).

Feasibility and Safety of Cardiomyotissue Implantation

The initial creation of the MI model with balloon occlusion was associated with 31% mortality secondary to ventricular fibrillation during balloon occlusion. Twenty-seven of 37 animals survived: 2 for male-female transplantation, 13 in the acute MI cohort (6 sham and 7 treated animals), and 12 in the healed infarct cohort (6 sham and 6 treated animals). There was no additional mortality associated with cardiomyotissue implantation. The animals tolerated both the biopsy of the basal septum and the anterior wall implantation without hypotension or sustained arrhythmias.

Histological Analysis and Male-Into-Female Transplantation Model

Histological analysis by hematoxylin and eosin staining confirmed the presence of extensive areas of infarction and fibrosis in the anteroseptal area. In the treated animals, all implants were identified and were viable (marked with 6–0 suture) in multiple tissue sections (Figure 2A). This was

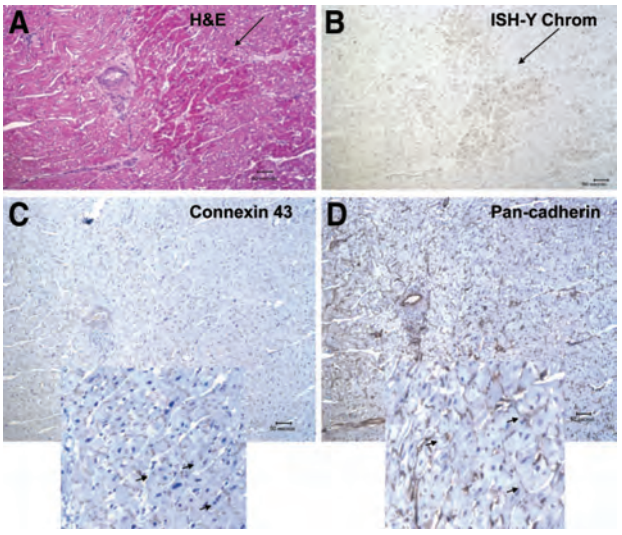

Figure 2. A, Histology. Hematoxylin and eosin–stained sections of an implant (arrow) within the infarct demonstrating good viability 2 weeks after implantation (×20). B, In situ hybridization for Y chromosome expression in the male-to-female implanted animals at 2 weeks after implantation (arrow). C, Anti-connexin43 (gap junction) immunohistochemical staining (×10) with high-power inset. D, Anti–pan-cadherin (desmosome) immunohistochemical staining in an adjacent section (×10) with high-power inset.

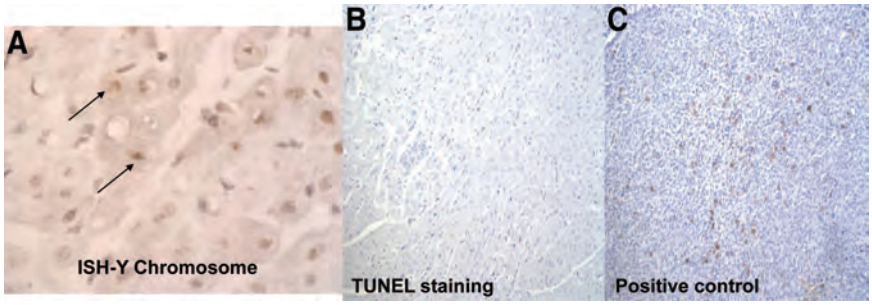

Figure 3. A, In situ hybridization Y chromosome–positive myocytes (arrow) outside the implant area dispersed among negative cells. B, Lack of apoptosis/TUNEL staining within the implant (×10). C, Positive control for TUNEL staining (×10).

confirmed by identification of male Y chromosome–positive implants in female recipients by in situ hybridization (Figure 2B). In addition, small infiltrates of inflammatory cells were identified at the implant site, most likely resulting from donors not HLA matched to recipients (only prednisone for immunosuppression). Staining for gap junctions with anti-connexin 43 antibody and for desmosomal junctions with anti–pan-cadherin antibody on sequential sections showed the presence of both gap junctions and desmosomes in the male-derived implants and connected these cells to surrounding female host tissue (Figure 2C and 2D). There was no evidence of apoptosis by TUNEL staining within the implant (Figure 3A and 3B). There was also no evidence of apoptosis in implants from acute and healed MI cohorts. In situ hybridization Y chromosome–positive cells were noted outside the implant area dispersed among negative cells, indicating possible migration and proliferation of implanted cells into the surrounding myocardium (Figure 3C).

Acute MI Cohort

MRI and Echocardiography Results

The perfusion ratio of anterior to septal wall was greater in the treated animals than in controls (1.2±0.01 versus 0.86±0.05; $P<0.01$; Figure 4A). Mean infarct volume (delayed enhancement) was smaller in treated than in control animals (2.2±0.5 versus 5.4±1.5; $P=0.04$; Figure 4B). Percent wall thickening was 9-fold greater in the anterior wall of treated animals compared with controls (60.5±40.2 versus 7.0±9.5; $P=0.069$). No such difference was seen in the nonimplanted septum (46.7±61 in treated versus 11.6±31 in controls; $P=0.4$). The difference in the overall EF between the 2 groups of 5% did not reach statistical significance (37.0±8.0% in treated animals versus 32.5±6.4% in controls; $P=0.28$). By echocardiography, the difference in overall EF between the 2 groups of 7% did not reach statistical significance (41±11% in treated animals versus 33±5% in controls; $P=0.16$).

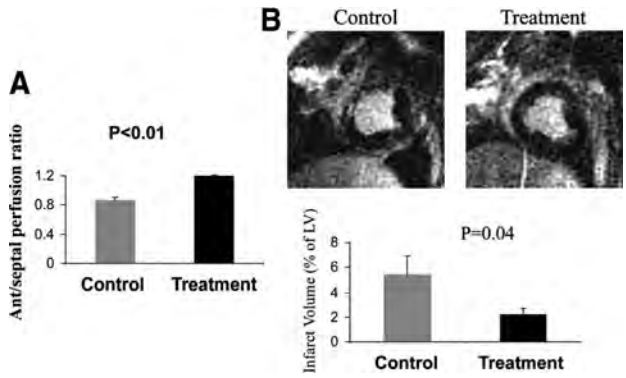

Figure 4. MRI. A, Treatment group (black bar) has a perfusion ratio >1.0 indicating greater perfusion in the treated anterior wall than in the untreated septal wall. Conversely, control animals (gray bar) had an anterior/septal wall perfusion ratio of <1.0, suggesting more severe compromise of perfusion to the anterior wall ($P<0.01$). B, Mean infarct volume as measured by delayed enhancement on cardiovascular magnetic resonance is lower in treated than in control animals.

Hemodynamics (dP/dt)

Contractility as measured by positive maximal dP/dt was greater in the treated animals compared with controls (1235±215 versus 817±817; $P<0.05$), indicating that the overall systolic myocardial function was improved in treated animals.

TTC Staining

The percent infarct size of the anterior wall area in the treated animals was 3-fold smaller than in controls (10.3±4.6 versus 28.9±5.8; $P<0.03$; Figure 5). There was no difference between the 2 groups in percent infarct size of the septal area (21.6±5.3 versus 21.5±2.5; $P=0.8$).

Healed MI Cohort

Echocardiographic Assessment of LV Function

Treated animals had the same EF at 2 and 4 week time points (49±6.5% versus 46±7.4%; $P=0.5$; Figure 6A). In contrast, EF decreased significantly in control animals between 2 and 4 weeks (50±10.4% versus 36±8.7%; $P=0.038$). Treated animals had significantly less decline in EF than controls (−3±4% versus −13±−4%; $P=0.003$).

Hemodynamics

Both systolic (positive dP/dt) and diastolic (negative dP/dt) function and LA pressures did not change in the treated animals between weeks 2 and 4 after infarction (Figure 6B). Control animals, on the other hand, had decreased positive dP/dt and negative dP/dt and increased left atrial pressures. In addition, treated animals had better hemodynamic parameter change between 2 and 4 weeks compared with controls (dP/dt: −6±61 versus −134±119, $P=0.04$; left atrial pressure: −1.4±1.32 versus 5.3±0.8 mmHg, $P<0.05$).

Morphometric Analysis

Percent infarct size in the anterior wall of treated animals was significantly smaller than control animals (21±11 versus 38±8; $P=0.006$). There was also a significant difference in

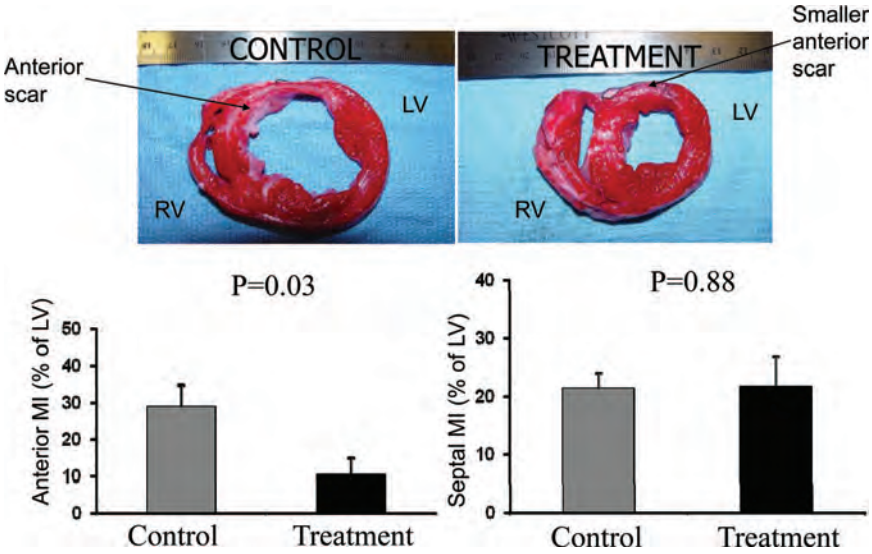

Figure 5. Measurement of the gross percent of MI in the anterior and septal regions of the myocardium by TTC staining. Percentage infarction in the anterior (treated) area is smaller in treated (black bar) than in control (gray bar) animals. Percentage infarction in the septal (untreated) area is the same in treated and control animals (right).

the infarct size in the untreated septum, suggesting a global effect of cardiomyotissue on myocardial salvage (16±11 versus 27±10; $P=0.02$), an effect not seen in acute MI cohort. TTC staining assessment was consistent between the 2 independent observers ($r=0.82$, $P=0.0005$).

Adjacent to the implants and within the infarct region, a 2-fold greater number of cells positive for mdr-1 were observed (Figure 7). C-kit+ cells, on the other hand, were more abundant in control animals. PECAM-1 staining identified increased numbers of capillaries and neovessels in the treated animals (Figure 8). In addition, neovessels appeared larger in caliber in the implanted animals, possibly suggesting a more advanced stage of angiogenesis and arteriolization.

Molecular Analysis

We explored the expression of MMP-2 and TIMP-2, known to be involved in remodeling after infarction.[28] Preserved myocardial function in treated animals correlated with 2-fold lower levels of MMP-2 and 2-fold higher levels of TIMP-2 (Figure 8).

Discussion

Cell-based therapies for myocardial regeneration have demonstrated variable initial results.[4–7,29] We have developed a new method of myocardial autotransplantation that obviates the need for cell culture and could be implemented during planned revascularization procedures. Implantation of cardiomyotissue appears to reduce infarct size and to prevent the decline in myocardial function after extensive anterior MI. This was evident in the preservation of EF, LV dimensions, and hemodynamic parameters and the decrease in infarct size in the treated animals compared with controls. In addition, implants remain viable and appear to express connexin 43

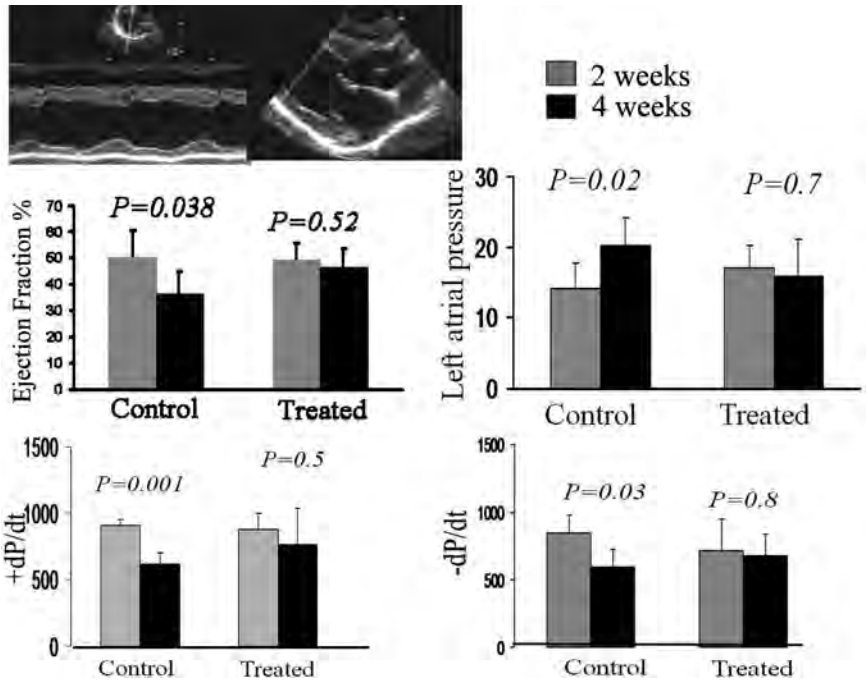

Figure 6. Top right, Cardiomyotissue implantation in the myocardial infarct zone 2 weeks after MI prevents deterioration in EF. EF remained the same in the treated animals between weeks 2 and 4. EF decreased in controls. Top left (bottom), Left-sided filling pressures show elevation in controls (14 to 20 mm Hg; $P=0.02$). Left atrial pressure remained normal in treated animals. Bottom, Hemodynamic assessment of contractility (dP/dt, right) and relaxation (−dP/dt, left). dP/dt and −dP/dt declined in the control animals. No such adverse effect was seen in the treated animals.

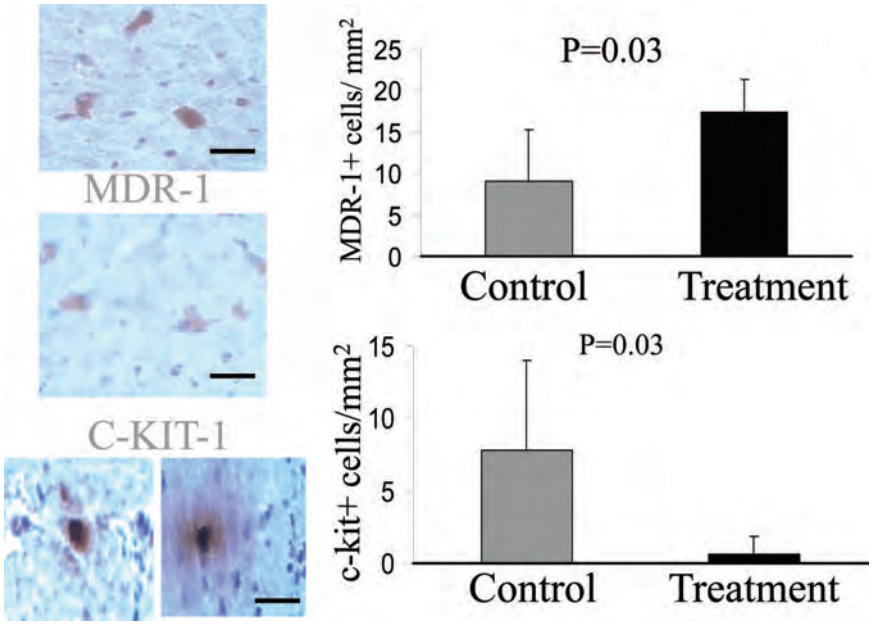

Figure 7. A, Adult cardiac stem cell quantification. Representative mdr-1 (top) and c-kit (bottom) staining in a treated animal (at ×20; bar=1 mm). Bar graphs represent cells per 1 mm^2 in treated animals vs controls. Higher numbers of mdr-1^+ cells (17 vs 9; P=0.038) but lower numbers of c-kit+ cells (1vs 8; P=0.034) were seen in treated animals.

and N-cadherin (gap junctions and desmosomes between the implant and surrounding myocardium). The effects in acute MI cohort were more robust than in the healed MI cohort, but this finding may be related in part to shorter treatment duration in this cohort. Our study was controlled for nonspecific effects of implantation by use of sham implants.

We propose that several mechanisms and intrinsic properties of whole-tissue implantation may be responsible for preventing the decline in myocardial function. It may avoid cell shearing and preserve tissue architecture and growth factor milieu within the extracellular matrix scaffold.[30] Fully developed cardiomyocytes within the implant may be more likely to remain viable and to contribute to increased contractility. The viability was poor in prior studies when cell suspensions were transferred.[19] In contrast, in our non–HLA-matched male-to-female implantation experiments, we observed good whole-implant viability without evidence of necrosis or apoptosis even in the presence of a low-level inflammatory reaction. In addition, myocardial implants appear to express both connexin 43 (gap junctions) and N-cadherin (desmosomes), which suggests electromechanical integration with the host myocardium, although this remains to be proven definitively in further studies. This finding may imply that unlike skeletal myoblasts that are electrically isolated,[31] myotissue implants will be less likely to cause ventricular arrhythmias.

In addition, we hypothesize that our biopsies may contain resident stem cells that may contribute to myocardial repair.[15,16] The overall contribution of resident stem cells to preservation of LV function in still uncertain, as is the

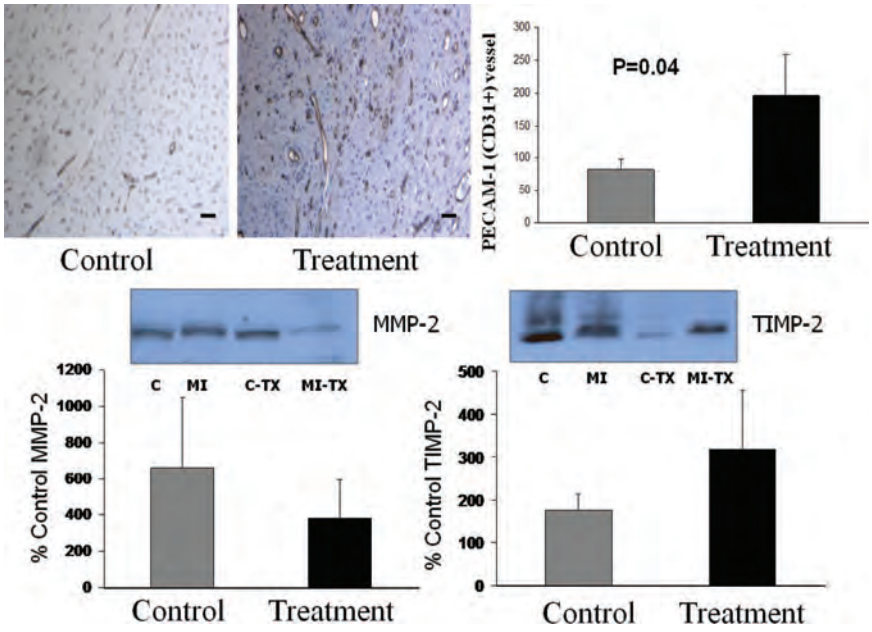

Figure 8. Top right, Increased vascularity in the implant-treated animals by PECAM-1 (CD31) staining. Vessels appeared more numerous and larger in caliber and lumen in treated animals. Magnification ×10. Top left, Quantification of the number of capillaries and neovessels by PECAM-1 (CD31) staining. Number of vessels was counted in a ×40 field and is represented per 1 mm^2. Implanted animals had 3-fold greater number of vessels (195±93 vs 82±65; P=0.04). Bottom, MMP protein expression. MMP-2 (left) and TIMP-2 (right) expression levels in infarcted (MI) and noninfarcted tissue (C) of treated (black) animals and controls (gray) with myotissue transplantation. MMP-2 levels tended to be 2-fold lower and TIMP-2 levels tended to be 2-fold higher in treated animals.

definition of a stem cell and its recognition based on cell surface markers. Furthermore, the differentiation potential of the adult cardiac stem cells may be limited by the trophic factor–impoverished milieu of the infarct.[15] By implanting the cardiac progenitor cells together with adjacent intact differentiated cardiomyocytes, however, we could have potentially provided them with those trophic factors necessary for differentiation. There was an overall increase in numbers of mdr-1^+ stem cells in the infarct zone of treated animals surrounding the implant sites. Mdr-1^+ cells have been shown to differentiate into myocytes, endothelial cells, smooth muscle cells, and fibroblasts.[27]

To explain the improvement in myocardial function in treated animals, we also looked at the postimplantation levels of PECAM-1 staining, which showed increased vessels with larger vessel caliber in treated animals. This may be suggestive of more advanced stage of angiogenesis with arteriolization in the treated animals. In the acute model of MI, we have been able to demonstrate increased perfusion by MRI imaging in animals treated with cardiomyotissue implantation compared with controls.

We observed that treated animals tended to have lower levels of MMP-2 and higher levels of TIMP-2, with more favorable hemodynamic parameters in treated animals. As demonstrated in murine models of MI, MMP-2 expression increases and is maintained for several weeks after infarction. MMP-2 knockout mice appear to have decreased dilation response after infarction.[32] TIMP knockout mice, on the other hand, have an exaggerated unfavorable remodeling with higher incidence of LV rupture and mortality.[33] Whether this effect of cardiomyotissue transplantation on MMP-2 and TIMP-2 expression is direct or indirect remains to be elucidated. The cardiomyotissue likely has higher compliance than the anterior myocardial scar and thus may improve remodeling via so-called matrix-associated myocardial stabilization and paracrine effects.[34] The reduction in infarct size by TTC staining and delayed enhancement MRI imaging seen in this model would argue, however, that this passive matrix myocardial stabilization is not the sole mechanism of improvement of myocardial function.

Finally, the effects of cardiomyotissue implantation can be contrasted with the effects of skin microorgan transplantation.[35] Although skin microorgan implantation improved perfusion, no effect on LV function was observed. In addition to improving perfusion, cardiomyotissue implantation resulted in improved LV function.

Limitations

This preliminary "proof of concept" study suffers from the limitation of lack of long-term follow-up and safety data. A major limitation was that randomization was not based on baseline infarct size and LV function. Furthermore, the worsening LV function in the acute MI control cohort conflicts with previous studies that surprisingly showed preserved LV function.[4] Such preclinical experiments are planned before this technology can be introduced into clinical trials. The efficacy in chronic ischemia and heart failure models will also have to be explored. In addition, testing of the performance of this technology in the context of maximal medical therapy with angiotensin-converting enzyme inhibitors that prevent adverse remodeling in the clinical setting will be important.

Conclusions

We presented here a novel approach to cellular therapy for MI, which involves septal biopsy and implantation of the intact tissue into the infarcted area. This novel implantation technique has low mortality in our swine model of MI and is technically simple to perform. These whole-biopsy implants were efficacious in preventing myocardial dysfunction as measured by MRI, echocardiography, and hemodynamic parameters and in decreasing infarct size. They obviate the need for tissue manipulation and culture. The implants are viable at 2 weeks after implantation and may be electromechanically coupled with the host myocardium. Further studies are needed to explore the beneficial mechanism of this novel technology.

Acknowledgments

We would like to thank Dr Anthony Rosenzweig for his advice and help with manuscript preparation and Justine Curley-Cohen for her help with histology.

Sources of Funding

This work was supported in part by National Institutes of Health grant HL63609, a Center for Integration of Medicine and Innovative Technology grant, and the DeBakey Foundation at Balamand University (Dr Laham).

Disclosures

The Beth Israel Deaconess Medical Center and 2 coauthors (Drs Wykrzykowska and Laham) hold patent rights to the technology described in this article. The other authors report no conflicts.

References

1. Chachques JC, Acar C, Herreros J, Trainini JC, Prosper F, D'Attellis N, Fabiani JN, Carpentier AF. Cellular cardiomyoplasty: clinical application. *Ann Thorac Surg*. 2004;77:1121–1130.
2. Dimmeler S, Zeiher AM, Schneider MD. Unchain my heart: the scientific foundations of cardiac repair. *J Clin Invest*. 2005;115:572–583.
3. Rosenzweig A. Cardiac cell therapy–mixed results from mixed cells. *N Engl J Med*. 2006;355:1274–1277.
4. Assmus B, Schachinger V, Teupe C, Britten M, Lehmann R, Dobert N, Grunwald F, Aicher A, Urbich C, Martin H, Hoelzer D, Dimmeler S, Zeiher AM. Transplantation of Progenitor Cells and Regeneration Enhancement in Acute Myocardial Infarction (TOPCARE-AMI). *Circulation*. 2002;106:3009–3017.
5. Wollert KC, Meyer GP, Lotz J, Ringes-Lichtenberg S, Lippolt P, Breidenbach C, Fichtner S, Korte T, Hornig B, Messinger D, Arseniev L, Hertenstein B, Ganser A, Drexler H. Intracoronary autologous bone-marrow cell transfer after myocardial infarction: the BOOST randomised controlled clinical trial. *Lancet*. 2004;364:141–148.
6. Perin EC, Dohmann HF, Borojevic R, Silva SA, Sousa AL, Mesquita CT, Rossi MI, Carvalho AC, Dutra HS, Dohmann HJ, Silva GV, Belem L, Vivacqua R, Rangel FO, Esporcatte R, Geng YJ, Vaughn WK, Assad JA, Mesquita ET, Willerson JT. Transendocardial, autologous bone marrow cell transplantation for severe, chronic ischemic heart failure. *Circulation*. 2003;107:2294–2302.
7. Smits PC, van Geuns RJ, Poldermans D, Bountioukos M, Onderwater EE, Lee CH, Maat AP, Serruys PW. Catheter-based intramyocardial injection of autologous skeletal myoblasts as a primary treatment of ischemic heart failure: clinical experience with six-month follow-up. *J Am Coll Cardiol*. 2003;42:2063–2069.
8. Kang HJ, Kim HS, Zhang SY, Park KW, Cho HJ, Koo BK, Kim YJ, Soo Lee D, Sohn DW, Han KS, Oh BH, Lee MM, Park YB. Effects of intracoronary infusion of peripheral blood stem-cells mobilised with granulocyte-colony stimulating factor on left ventricular systolic function

and restenosis after coronary stenting in myocardial infarction: the MAGIC cell randomised clinical trial. *Lancet*. 2004;363:751–756.
9. Carr CA, Stuckey DJ, Tatton L, Tyler DJ, Hale SJ, Sweeney D, Schneider JE, Martin-Rendon E, Radda GK, Harding SE, Watt SM, Clarke K. Bone marrow-derived stromal cells home to and remain in the infarcted rat heart but fail to improve function: an in vivo cine-MRI study. *Am J Physiol Heart Circ Physiol*. 2008;295:H533–542.
10. Smart N, Riley PR. The stem cell movement. *Circ Res*. 2008;102: 1155–1168.
11. van der Bogt KE, Sheikh AY, Schrepfer S, Hoyt G, Cao F, Ransohoff KJ, Swijnenburg RJ, Pearl J, Lee A, Fischbein M, Contag CH, Robbins RC, Wu JC. Comparison of different adult stem cell types for treatment of myocardial ischemia. *Circulation*. 2008;118:S121–129.
12. Beltrami AP, Barlucchi L, Torella D, Baker M, Limana F, Chimenti S, Kasahara H, Rota M, Musso E, Urbanek K, Leri A, Kajstura J, Nadal-Ginard B, Anversa P. Adult cardiac stem cells are multipotent and support myocardial regeneration. *Cell*. 2003;114:763–776.
13. Nadal-Ginard B, Kajstura J, Anversa P, Leri A. A matter of life and death: cardiac myocyte apoptosis and regeneration. *J Clin Invest*. 2003;111: 1457–1459.
14. Leri A, Kajstura J, Anversa P. Cardiac stem cells and mechanisms of myocardial regeneration. *Physiol Rev*. 2005;85:1373–1416.
15. Dawn B, Stein AB, Urbanek K, Rota M, Whang B, Rastaldo R, Torella D, Tang XL, Rezazadeh A, Kajstura J, Leri A, Hunt G, Varma J, Prabhu SD, Anversa P, Bolli R. Cardiac stem cells delivered intravascularly traverse the vessel barrier, regenerate infarcted myocardium, and improve cardiac function. *Proc Natl Acad Sci U S A*. 2005;102:3766–3771.
16. Kajstura J, Rota M, Whang B, Cascapera S, Hosoda T, Bearzi C, Nurzynska D, Kasahara H, Zias E, Bonafe M, Nadal-Ginard B, Torella D, Nascimbene A, Quaini F, Urbanek K, Leri A, Anversa P. Bone marrow cells differentiate in cardiac cell lineages after infarction independently of cell fusion. *Circ Res*. 2005;96:127–137.
17. Laham RJ, Rezaee M, Post M, Sellke FW, Braeckman RA, Hung D, Simons M. Intracoronary and intravenous administration of basic fibroblast growth factor: myocardial and tissue distribution. *Drug Metab Dispos*. 1999;27:821–826.
18. Laham RJ, Post M, Rezaee M, Donnell-Fink L, Wykrzykowska JJ, Lee SU, Baim DS, Sellke FW. Transendocardial and trans-epicardial intramyocardial FGF-2 administration: Myocardial and Tissue Distribution. *Drug Metab Dispos*. 2005;33:1101–1107.
19. Muller-Ehmsen J, Peterson KL, Kedes L, Whittaker P, Dow JS, Long TI, Laird PW, Kloner RA. Rebuilding a damaged heart: long-term survival of transplanted neonatal rat cardiomyocytes after myocardial infarction and effect on cardiac function. *Circulation*. 2002;105:1720–1726.
20. Christman KL, Vardanian AJ, Fang Q, Sievers RE, Fok HH, Lee RJ. Injectable fibrin scaffold improves cell transplant survival, reduces infarct expansion, and induces neovasculature formation in ischemic myocardium. *J Am Coll Cardiol*. 2004;44:654–660.
21. Murry CE, Soonpaa MH, Reinecke H, Nakajima H, Nakajima HO, Rubart M, Pasumarthi KB, Virag JI, Bartelmez SH, Poppa V, Bradford G, Dowell JD, Williams DA, Field LJ. Haematopoietic stem cells do not transdifferentiate into cardiac myocytes in myocardial infarcts. *Nature*. 2004;428:664–668.
22. Balsam LB, Wagers AJ, Christensen JL, Kofidis T, Weissman IL, Robbins RC. Haematopoietic stem cells adopt mature haematopoietic fates in ischaemic myocardium. *Nature*. 2004;428:668–673.
23. Pearlman JD, Laham RJ, Simons M. Coronary angiogenesis: detection in vivo with MR imaging sensitive to collateral neocirculation: preliminary study in pigs. *Radiology*. 2000;214:801–807.
24. Royse CF, Royse AG, Bharatula A, Lai J, Veltman M, Cope L, Kumar A. Substernal epicardial echocardiography: a recommended examination sequence and clinical evaluation in patients undergoing cardiac surgery. *Ann Thorac Surg*. 2004;78:613–619; discussion 619.
25. Uematsu M, Gaudette GR, Laurikka JO, Levitsky S, McCully JD. Adenosine-enhanced ischemic preconditioning decreases infarct in the regional ischemic sheep heart. *Ann Thorac Surg*. 1998;66:382–387.
26. Vivaldi MT, Kloner RA, Schoen FJ. Triphenyltetrazolium staining of irreversible ischemic injury following coronary artery occlusion in rats. *Am J Pathol*. 1985;121:522–530.
27. Urbanek K, Quaini F, Tasca G, Torella D, Castaldo C, Nadal-Ginard B, Leri A, Kajstura J, Quaini E, Anversa P. Intense myocyte formation from cardiac stem cells in human cardiac hypertrophy. *Proc Natl Acad Sci U S A*. 2003;100:10440–10445.
28. Chen J, Tung CH, Allport JR, Chen S, Weissleder R, Huang PL. Near-infrared fluorescent imaging of matrix metalloproteinase activity after myocardial infarction. *Circulation*. 2005;111:1800–1805.
29. Strauer BE, Brehm M, Zeus T, Kostering M, Hernandez A, Sorg RV, Kogler G, Wernet P. Repair of infarcted myocardium by autologous intracoronary mononuclear bone marrow cell transplantation in humans. *Circulation*. 2002;106:1913–1918.
30. Leor J, Aboulafia-Etzion S, Dar A, Shapiro L, Barbash IM, Battler A, Granot Y, Cohen S. Bioengineered cardiac grafts: A new approach to repair the infarcted myocardium? *Circulation.* 2000;102:III56–61.
31. Reinecke H, MacDonald GH, Hauschka SD, Murry CE. Electromechanical coupling between skeletal and cardiac muscle. Implications for infarct repair. *J Cell Biol*. 2000;149:731–740.
32. Hayashidani S, Tsutsui H, Ikeuchi M, Shiomi T, Matsusaka H, Kubota T, Imanaka-Yoshida K, Itoh T, Takeshita A. Targeted deletion of MMP-2 attenuates early LV rupture and late remodeling after experimental myocardial infarction. *Am J Physiol Heart Circ Physiol*. 2003;285:H1229–1235.
33. Ikonomidis JS, Hendrick JW, Parkhurst AM, Herron AR, Escobar PG, Dowdy KB, Stroud RE, Hapke E, Zile MR, Spinale FG. Accelerated LV remodeling after myocardial infarction in TIMP-1-deficient mice: effects of exogenous MMP inhibition. *Am J Physiol Heart Circ Physiol*. 2005; 288:H149–158.
34. Wall S, Walker J, Healy K, Ratcliffe M, Guccione J. Theoretical Impact of the Injection of Material Into the Myocardium: A Finite Element Model Simulation. *Circulation*. 2006;114:2627–2635.
35. Voisine P, Rosinberg A, Wykrzykowska JJ, Shamis Y, Wu GF, Appelbaum E, Li J, Sellke FW, Pinto D, Gibson CM, Mitrani E, Laham RJ. Skin-derived microorgan autotransplantation as a novel approach for therapeutic angiogenesis. *Am J Physiol Heart Circ Physiol*. 2008;294: H213–219.

CLINICAL PERSPECTIVE

Myocardial infarction and the resultant left ventricular dysfunction remain a leading cause of mortality and morbidity. Different therapies for myocardial regeneration have been investigated with varying results and no definitive beneficial effects. Concomitantly, the intrinsic regenerative potential of the myocardium has been increasingly recognized. Adult cardiac stem cells injected into vasculature of rats after myocardial infarction are able to differentiate into cardiomyocytes and arterioles. In addition, it has been increasingly recognized that the delivery modality is a key limiting step in attempts at myocardial regeneration and angiogenesis with poor survival of transplanted cells (possibly related to "milieu") and limited deposition and retention of injected cytokines. This, coupled with mounting evidence relative to the lack of transdifferentiation potential of adult non–cardiac-derived stem cells, warrants a novel approach to myocardial regeneration. We have developed a novel approach to adult cardiomyocyte transplantation using autologous transplantation of normal cardiac myocardial tissue into areas of acute or healed myocardial infarction. Our results suggest a reduction in infarct size, improved left ventricular function and hemodynamics, improved remodeling, and possibly regeneration of damaged myocardial with resident stem cells from transplanted tissue.

Appendix 1 (supplemental information)

Description of the bioptome:

The bioptome performs a gun biopsy of the septum by exposing the sharp blade shown below within the tissue. As the bioptome window is placed in a closed position the biopsy material is protected inside. The bioptome can then be reinserted into the anterior wall infract/scar area and the bioptome window is opened again exposing the biopsy. The bioptome is then turned 180 degrees such that the biopsy is removed out of the bioptome, deposited in the scar and not dragged back as the bioptome is retracted back. This bioptome was in this case a biopsy and an implantation device.

MRI sequences for myocardial perfusion assessment:

The animals were placed in the right antecubital position, and a phased-array cardiac coil was placed around the chest. Mechanical ventilation and gaseous anesthesia was continued during scanning. Scout images were obtained to determine the short and long axis views of the heart. Fast imaging employing steady-state acquisition (FIESTA) pulse sequence was used to assess global and regional LV function. Short axis cine images were acquired with ECG gating with breathhold. The heart was imaged from base to apex with eight to ten LV short axis slices. The image parameters were as follows: TR/TE=3.8/1.7ms, flip angle was 45^{o}, 224 × 224 matrix, 8 mm slice thickness no gap, bandwidth 125 kHz, field of view 26 cm and 1 NEX. MR Perfusion images were acquired in three slices each matched to short axis cine slice, representing the basal, midventricular, and apical myocardial segments, with ECG gated and non-breathhold fast gradient echo-echo train with multi phase (FGRET-MP) pulse sequence. After three to five heart beat initiation of the sequence as the baseline images, first-pass perfusion images were acquired after intravenous injection of 0.1 mmol/kg bodyweight gadolinium-DTPA (Magnevist, Berlex Laboratories, NJ) which was injected at

the rate of 3.0 ml/sec, followed by a 20 ml saline flush at the rate of 3.0 ml/sec by an infusion pump, total 50 phases were acquired each slice. Imaging parameters included the following: TR/TE=9.3/1.8 ms, inversion time 160 ms, echo train length of four, 128 × 128 matrix, flip angle 25^{o}, 26 cm field of view, 8 mm slice thickness, 2 mm section spacing, 125 kHz bandwidth.

Infarct size was analyzed by using the delayed enhancement CMR technique. After completion of the cine and first-pass perfusion imaging, delayed enhancement images were acquired 15 min after a bolus injection 0.2 mmol/kg bodyweight gadolinium-DTPA.[1] By using an ECG-gated, breathhold, 2D interleaved, inversion recovery, fast-gradient recoiled echo pulse sequence. A total of 8-10 continuous short-axis slices were prescribed to cover the entire LV from base to apex. Imaging parameters were as follow: TR/TE=6.7/3.2 ms, inversion recovery time 180 ~ 220 ms, flip angle= 20^{o}, 256 × 192 matrix, 8 mm slice thickness / no gap, bandwidth 31.25 kHz, 26 cm field of view and 2 NEX, Inversion recovery time was adjusted as needed to null the normal myocardium.

All the measurements were analyzed offline by an independent blinded investigator with commercial software (MASS by Medis Inc., Netherlands). For the myocardial perfusion analysis, short axis images were sorted according to slice position and acquisition time, the LV endocardial and epicardial contours were draw manually and six equiangular segments (anterior, antero-lateral, infero-lateral, inferior, infero-septal, antero-septal) per slice were generated automatically, the anterior septal insertion of the right ventricle as a reference point. The upslope of myocardial signal in six segments were divided by the upslope of the signal in the left ventricular cavity, which was regarded as a measure of the input function.[2] Infarct size was determined as a percentage of LV (%LV) as the total of hyperenhanced pixels from each of the 8-10 continuous short axis slices divided by the total number of pixels within the LV myocardium multiplied by 100. The area of delayed-enhancement was defined as the pixels where the signal intensity differed by + 2 SDs from the signal enhancement in the remote myocardium (inferior wall) in the same slice.

1. Simonetti OP, Kim RJ, Fieno DS, et al. An improved MR imaging technique for the visualization of myocardial infarction. *Radiology.* Jan 2001;218(1):215-223.

2. Schwitter J, Nanz D, Kneifel S, et al. Assessment of myocardial perfusion in coronary artery disease by magnetic resonance: a comparison with positron emission tomography and coronary angiography. *Circulation.* May 8 2001;103(18):2230-2235.

Figure 1: Implantation: Right Ventricular (RV) free wall was incised and a bioptome (Cook Inc) introduced through an 8 Fr sheath. 6-10 biopsies were obtained from the ventricular basal septum. The same bioptome was used as an implantation device to deposit implants into the anterior myocardial scar. Sham operated animals also underwent a right thoracotomy and septal biopsy but an empty bioptome was introduced into the anterior wall scar.